

## Dating by Cosmogenic Nuclides

**Paul R Bierman**, Department of Geology, University of Vermont, Burlington, VT, United States

**Adrian M Bender**, US Geological Survey, Alaska Science Center, Anchorage, AK, United States

**Andrew J Christ, Lee B Corbett, and Christopher T Halsted**, Department of Geology, University of Vermont, Burlington, VT, United States

**Eric W Portenga**, Department of Geography and Geology, Eastern Michigan University, Ypsilanti, MI, United States

**Amanda H Schmidt**, Geology Department, Oberlin College, Oberlin, OH, United States

© 2021 Published by Elsevier Ltd.

<b>Introduction</b>	<b>101</b>
<b>Commonly Used Cosmogenic Nuclides</b>	<b>104</b>
<b>Sample Preparation</b>	<b>105</b>
<b>Applications</b>	<b>105</b>
Erosion	105
Outcrop Erosion Rates	105
Basin-Averaged Erosion Rates	107
Dating	108
Simple Glacial Dating	108
Simple Burial Dating	109
Isochron Burial Dating	109
Importance of Nuclide Inheritance for Dating	110
Complex Exposure Histories	111
<b>Sediment Sourcing and Tracing</b>	<b>112</b>
Storms, Wet Seasons, and Reproducibility Over Time	113
Analysis of Deep-Sea Sediment	114
<b>What Will the Future Bring?</b>	<b>114</b>
<b>Further Reading</b>	<b>115</b>

### Glossary

**Accelerator mass spectrometer (AMS)** Isotope ratio mass spectrometer using negative ions and multiple acceleration stages with filters to separate ions of similar mass.

**Cosmogenic** Produced by the interaction of cosmic rays.

**Holocene** An epoch of geologic time, spanning ~11.7 ka to present.

**Landforms** Distinctive features on Earth's surface.

**Meteoritic** Produced in the atmosphere.

**Miocene** An epoch of geologic time, spanning ~23.0–5.3 Ma.

**Nuclide (and/or radionuclide)** Element with specific number of neutrons and protons.

**Nuclide inheritance** Presence of nuclides produced prior to current period of cosmic ray exposure.

**Pleistocene** An epoch of geologic time, spanning ~2.6 My to ~11.7 Ky ago.

**Pliocene** An epoch of geologic time, spanning ~5.3–2.6 My ago.

**Primary cosmic rays (or ray flux)** Primarily protons with high energy interacting with atmospheric gasses and originating from the galaxy outside our solar system.

**Production pathways** Different nuclear and cosmic ray interactions capable of producing cosmogenic nuclides.

**Secondary cosmic rays (or ray flux)** Primarily neutrons formed by interaction of primary cosmic rays with atmospheric gasses.

### Abbreviations

**ka** Kilo-annum; thousand years ago

**Ky** Thousand years

**Ma** Mega-annum; million years ago

**My** Million years

## Introduction

Cosmogenic nuclides provide a direct means of measuring the residence time of rock, sediment, and soil at and near Earth's dynamic surface. Measurements of nuclide concentrations in bedrock, detrital sediment, saprolite, sedimentary deposits, and soils have been used to determine the rates and dates of a diverse suite of surface and near-surface processes including erosion, glaciation, faulting, sedimentation, river incision, and soil formation.

Cosmogenic nuclides are formed by the interaction of cosmic rays, primarily secondary neutrons, with other target particles, such as oxygen atoms (Fig. 1). These cosmic rays originate as protons in the galaxy outside our solar system. Nuclide production may occur in the atmosphere (i.e., meteoric nuclides) or in inorganic mineral lattices (i.e., in situ nuclides). In situ nuclides such as  $^{10}\text{Be}$ ,  $^{26}\text{Al}$ ,  $^{14}\text{C}$ , and  $^{21}\text{Ne}$  are often measured in quartz ( $\text{SiO}_2$ ) for several reasons. Quartz is a common mineral in earth materials that is resistant to weathering. Si and O are target atoms for cosmic ray bombardment and the simple, consistent chemical composition of quartz means nuclide production rates do not depend on mineral composition. Several cosmogenic radionuclides, including  $^{10}\text{Be}$ ,  $^{14}\text{C}$ ,  $^{26}\text{Al}$ , and  $^{36}\text{Cl}$ , are commonly measured using ultrasensitive accelerator mass spectrometers (AMS). The stable cosmogenic nuclides,  $^3\text{He}$  and  $^{21}\text{Ne}$ , are measured using smaller, traditional noble gas mass spectrometers.

Cosmogenic nuclide production rates are low (on the order of several to hundreds of atoms per gram per year, Table 1) and vary by latitude and altitude of the sample site (Fig. 2). Geographic variability in nuclide production rates is controlled by the magnitude of the secondary cosmic ray flux; the neutrons produced as cosmic ray protons interact with atmospheric gases. The flux of these neutrons is affected by both atmospheric depth (or altitude) and the orientation of Earth's geomagnetic field lines. The flux of

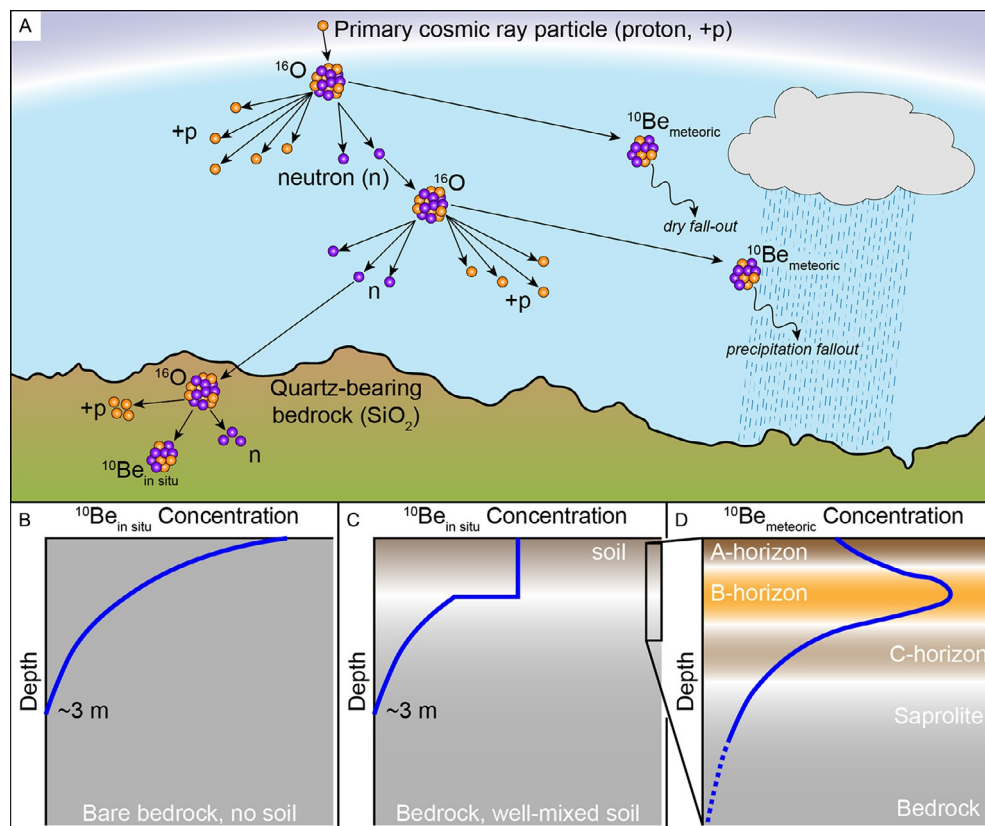


**Fig. 1** (A) A simplified illustration of the production of the cosmogenic nuclide, beryllium-10 ( $^{10}\text{Be}$ ), by spallation reactions between primary cosmic rays (protons,  $+p$ ) and secondary neutrons ( $n$ ) with target 16-oxygen ( $^{16}\text{O}$ ) atoms in the atmosphere and in quartz-bearing bedrock (modified from von Blanckenburg and Willenbring, 2014).  $^{10}\text{Be}$  produced in situ via spallation of  $^{16}\text{O}$  in quartz ( $\text{SiO}_2$ )-bearing bedrock remains locked in the quartz mineral crystal structure ( $^{10}\text{Be}_{\text{in situ}}$ ) whereas  $^{10}\text{Be}$  produced in the atmosphere is referred to as meteoric  $^{10}\text{Be}$  ( $^{10}\text{Be}_{\text{meteoric}}$ ) as it falls to Earth's surface as dry fallout or with precipitation. The production of other cosmogenic nuclides ( $^3\text{He}$ ,  $^{10}\text{Be}$ ,  $^{14}\text{C}$ ,  $^{21}\text{Ne}$ ,  $^{26}\text{Al}$ , and  $^{36}\text{Cl}$ ), the production of  $^{10}\text{Be}$  by muons (Gosse and Phillips, 2001), and the production of  $^{10}\text{Be}_{\text{in situ}}$  in non-quartz minerals are not shown for clarity. (B)  $^{10}\text{Be}_{\text{in situ}}$  production in bedrock decreases exponentially with depth, such that at bedrock depths  $> \sim 3$  m, few atoms of  $^{10}\text{Be}_{\text{in situ}}$  are produced through spallogenic reactions;  $^{10}\text{Be}_{\text{in situ}}$  production by muon capture occurs at greater depths (Fig. 3). The depth profile of  $^{10}\text{Be}_{\text{in situ}}$  through time reflects a balance between the bedrock exposure history, the production rate of  $^{10}\text{Be}_{\text{in situ}}$ , radioactive decay of  $^{10}\text{Be}_{\text{in situ}}$  ( $t_{1/2} \approx 1.36$  My), and the erosion rate of the bedrock surface. (C) In landscapes where bedrock is blanketed by a mantle of well-mixed soil,  $^{10}\text{Be}_{\text{in situ}}$  throughout the soil profile often has homogenous concentration the result of soil stirring (Brown et al., 1995). (D) Upon delivery to Earth's surface,  $^{10}\text{Be}_{\text{meteoric}}$  adsorbs strongly to sediment and soil particles; desorption is rare in soils with  $\text{pH} > 4$ .  $^{10}\text{Be}_{\text{meteoric}}$  accumulation is often greater in well-developed B horizons a high concentration of clays and fine particles have a greater adsorption surface area per unit soil volume (Graly et al., 2010).

**Table 1** Cosmogenic nuclides and properties after von Blanckenburg and Willenbring (2014).

Nuclide	Half-life (My)	Production rate <sup>a</sup>	Minerals used	
In situ	<sup>3</sup> He	Stable	75–120	Olivine, pyroxene
	<sup>10</sup> Be	1.4	4–5	Quartz
	<sup>14</sup> C	$5.7 \times 10^{-4}$	18–20	Quartz
	<sup>26</sup> Al	0.7	35	Quartz
	<sup>21</sup> Ne	Stable	18–21	Quartz, olivine, pyroxene
	<sup>36</sup> Cl <sup>b</sup>	0.3	70 (Ca) 200 (K)	Calcite (Ca) K-feldspar (K)
Meteoric	<sup>10</sup> Be	1.4	0.2–2	All fine-grained, reactive surfaces (clay, Fe-hydroxides)

<sup>a</sup>Production rate at sea level and high latitude. Units of atoms/g per year for in situ production; units of  $10^6$  atoms/(cm<sup>2</sup>·year) for meteoric reflect nuclide flux at Earth’s surface.

<sup>b</sup>Production depends on amount of Ca and K in the mineral.

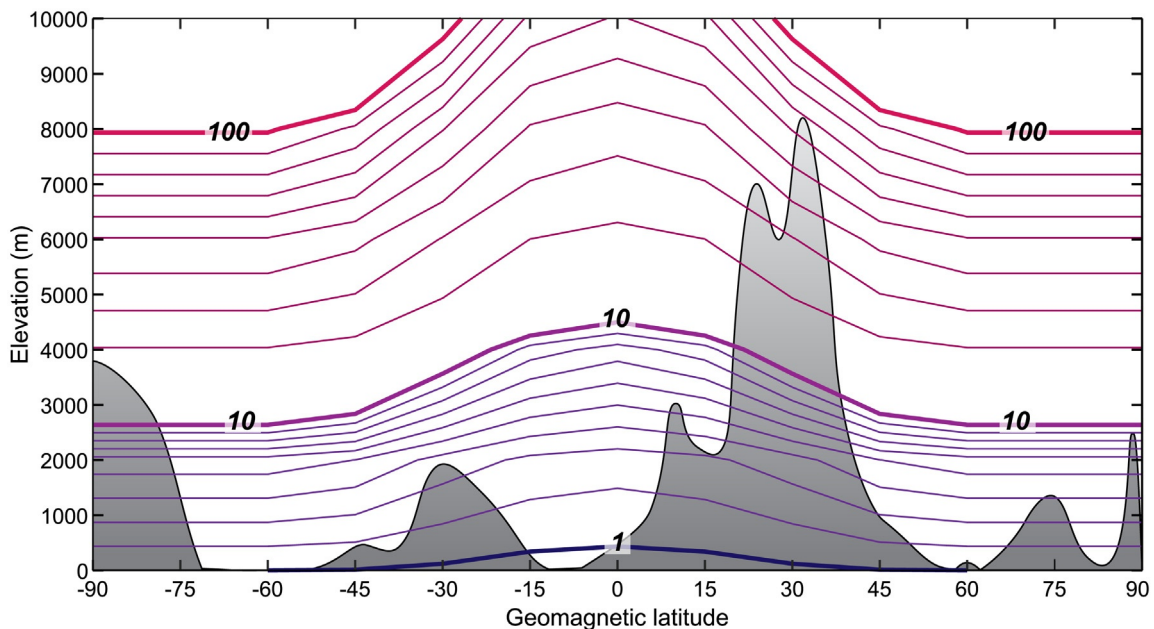


**Fig. 2** Production rate scaling with geomagnetic latitude and elevation after Lal (1991). Logarithmically spaced contour lines show the <sup>10</sup>Be production rate relative to the sea level, high latitude (60°) production. Grayscale topography is hypothetical and shown for reference.

cosmic ray neutrons is attenuated by the atmosphere; thus, cosmogenic nuclide production rates are much greater at high elevations than at sea level. For example, the production rate of <sup>10</sup>Be in quartz is tens of atoms per gram at a few thousand meters elevation and only a few atoms per gram at sea level.

Cosmogenic nuclide production rates are higher at the poles than at the equator because of Earth’s geomagnetic field. Primary cosmic ray protons, originating from outside the solar system (and thus termed galactic) are charged particles. They are deflected more efficiently at low latitudes, where they cross perpendicular to Earth’s magnetic field lines. At the poles, primary cosmic ray protons travel parallel to the field lines and thus are not deflected. As a result, cosmogenic nuclide production rates at sites above 60° latitude are nearly twice those at the equator. This dependence of production rates on sample location latitude and altitude means that detection limits, when considered in terms of exposure time, vary by location. To place this in context, nuclides produced during 100 years of surface exposure on a mountaintop of the Alps would be detectable, whereas it might take 1000 years to build up sufficient cosmogenic nuclides to detect exposure along an equatorial coastline.

Cosmic rays are absorbed as they penetrate rock and soil (Fig. 3). After penetrating a meter of rock, less than 20% of the cosmic ray neutron flux remains. With depth, small rarely interacting cosmic ray particles called muons do most of the production. Production of cosmogenic nuclides continues to depths of tens of meters in rock but at very low rates. When such rock is eroded, for example by glaciers, boulders and sand derived from deep erosion can contain enough cosmogenic nuclides to increase resulting exposure ages in exposed samples by decades to centuries.

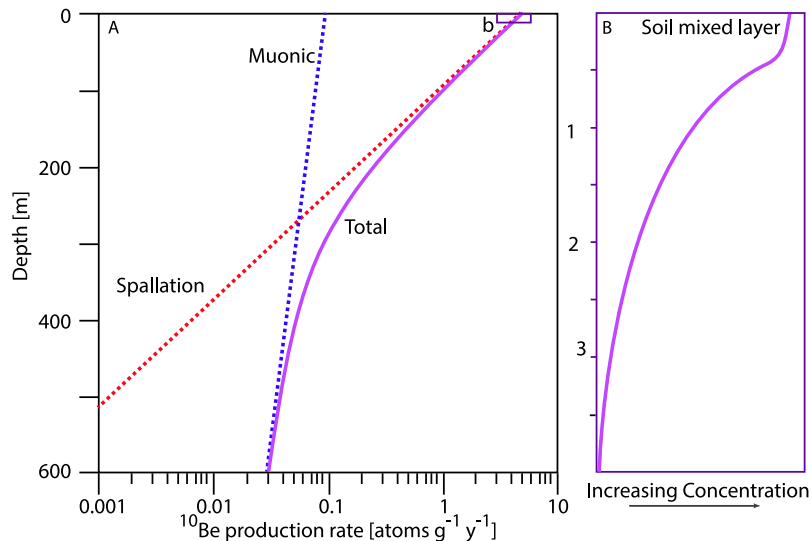


**Fig. 3** Profile showing production of  $^{10}\text{Be}$  in quartz with depth and the relative influence of spallation and muogenic production, (A) is modified from Gosse and Phillips (2001) and (B) shows enlarged typical profile for top 3 m of soil.

### Commonly Used Cosmogenic Nuclides

The nuclide  $^{10}\text{Be}$ , with a half-life of  $\sim 1.39$  My, is the most widely measured cosmogenic isotope. It is produced both in the atmosphere (meteoric  $^{10}\text{Be}$ ) as cosmic ray neutrons interact with oxygen and nitrogen nuclei and in near-surface materials (in situ  $^{10}\text{Be}$ ). Meteoric  $^{10}\text{Be}$  reaches Earth's surface as dry fall, or when scavenged by rain, and rapidly adheres to mineral surfaces where it becomes incorporated in coatings on mineral grains. In situ  $^{10}\text{Be}$  is produced within minerals through cosmic ray penetration and is usually measured in quartz. The distribution of meteoric  $^{10}\text{Be}$  is controlled by a combination of geological, chemical, physical, and biological processes, complicating interpretive models and making the results less certain. In contrast, the amount and concentration of in situ produced  $^{10}\text{Be}$  is more predictable and therefore more easily interpretable than the concentration of meteoric  $^{10}\text{Be}$ .

The cosmogenic nuclide  $^{26}\text{Al}$  has primarily been measured in quartz, with a small number of measurements in olivine and just a few in calcite. It is produced in quartz at the Earth's surface at a rate about seven times greater than  $^{10}\text{Be}$ . It is almost always measured along with  $^{10}\text{Be}$  because both nuclides are extracted in the same laboratory process from quartz. Once separated from other elements,  $^{26}\text{Al}/^{27}\text{Al}$  is measured by AMS. Recent advancements in AMS techniques increased the sensitivity of  $^{26}\text{Al}$  measurements tenfold, so that analytic detection limits are now similar to those for  $^{10}\text{Be}$ . Because  $^{26}\text{Al}$  has a half-life of 705 Ky (about half as long as  $^{10}\text{Be}$ ), it is particularly useful for dating sediment burial when paired with  $^{10}\text{Be}$ . For example, if sediment samples that have been exposed are then buried, the in situ  $^{26}\text{Al}$  decays more rapidly than the in situ  $^{10}\text{Be}$ . This discordance allows computation of the duration of post-burial decay, and thus the timing of burial.

The nuclide  $^{36}\text{Cl}$ , with a half-life of 301 Ky has been measured in both whole rock samples (which allows it to be used anywhere, independent of lithology) and in mineral separates, primarily feldspars. Interpreting in situ cosmogenic  $^{36}\text{Cl}$  data is more complicated than some other cosmogenic nuclides because  $^{36}\text{Cl}$  has a variety of production pathways. These pathways each have different depth/production relationships and the peak of one pathway is actually tens of centimeters below the surface. As a result,  $^{36}\text{Cl}$  production rates remain difficult to precisely and accurately define, thus limiting the application of  $^{36}\text{Cl}$ . However, analysis of  $^{36}\text{Cl}$  in mineral separates significantly reduces the uncertainty of data interpretation, and thus represents the potential to expand the types of rocks in which cosmogenic nuclides can be measured and interpreted.

The nuclide  $^{14}\text{C}$ , the widely known chronometer used for decay dating of organic material and inorganic sediment, is also produced in situ in surface materials. Extracting in situ  $^{14}\text{C}$  is complicated by the high potential for contamination from atmospheric  $^{14}\text{CO}_2$ . In addition to the difficulties associated with extraction, analysis of in situ  $^{14}\text{C}$  for surficial processes is further complicated because it is produced at greater depths below the surface than other nuclides. Despite extraction difficulties and interpretation uncertainties, in situ  $^{14}\text{C}$  is a useful tool due to its comparatively short half-life of 5.7 Ky. In situ  $^{14}\text{C}$  is particularly useful when its concentration is measured in the same sample as a long-lived cosmogenic radionuclide (such as  $^{10}\text{Be}$ ). This pairing allows the detection of surface erosion rate changes, complex surface exposure histories, or events of mass removal such as loss of slabs from rock surfaces within the Holocene to late Pleistocene. For example, paired  $^{14}\text{C}$ - $^{10}\text{Be}$  concentrations measured in river sand have recently been used to infer landslide frequency in catchments upstream of the sample collection site. In glacial settings, where surface material is covered by cold-based non-erosive glacier ice, in situ  $^{14}\text{C}$  can be paired with  $^{10}\text{Be}$  to detect if and how long the surface material was exposed prior to the most recent glaciation.

The stable noble gas cosmogenic nuclides,  $^3\text{He}$  and  $^{21}\text{Ne}$ , have been measured in a wider variety of minerals than the cosmogenic radionuclides. Production rates for  $^3\text{He}$  are high (75–120 atoms per gram per year) and the measurements require

less sample mass (<1 g) and far less chemical and physical pre-treatment than do the cosmogenic radionuclides. However,  $^3\text{He}$  rapidly diffuses from minerals such as quartz, limiting its reliable geochronologic application to minerals such as olivine.  $^{21}\text{Ne}$  can be measured in small masses of quartz and other minerals, but reliable quantification of cosmogenic  $^{21}\text{Ne}$  is challenged by the large volumes of  $^{21}\text{Ne}$  produced by alpha particles in rock (emitted from U and Th), which produce  $^{21}\text{Ne}$  as they interact with oxygen in minerals.

## Sample Preparation

Sample preparation for all in situ cosmogenic nuclides, except whole-rock  $^{36}\text{Cl}$ , begins with the isolation of the mineral phase of interest (usually quartz or feldspar). Such isolation is most frequently done using a combination of magnetic separation, density separation, selective acid etching, and handpicking. Noble gas analysis ( $^3\text{He}$  and  $^{21}\text{Ne}$ ) requires a gram or less of purified minerals,  $^{14}\text{C}$  requires grams, and the other nuclides are most precisely measured in separates of 10 g or more.

Most cosmogenic radionuclide analyses rely on the principle of isotopic dilution, during which the non-cosmogenic stable isotope is added to a sample artificially at the beginning of sample processing. For example, for the in situ  $^{10}\text{Be}$  system,  $^9\text{Be}$  is added before the purified quartz is digested. The addition of the non-cosmogenic isotope provides sufficient mass of material for preparation and analysis, and also enables accelerator mass spectrometry, which relies upon measuring the ratio of two isotopes. Accelerators measure  $^{10}\text{Be}/^9\text{Be}$ , which can be converted to the number of atoms of  $^{10}\text{Be}$  because the number of atoms of  $^9\text{Be}$  added is known.

For in situ  $^{10}\text{Be}$  and  $^{26}\text{Al}$ , sample preparation relies upon the isolation of Be and Al from purified mineral separates, usually quartz. Although methods vary between laboratories, the approach is usually characterized by complete digestion of the purified quartz in hydrofluoric acid followed by the removal of other interfering elements (chiefly Fe, Ti, and Mg) as well as the separation of Be and Al by column chromatography (Fig. 4). For meteoric  $^{10}\text{Be}$ , sample preparation includes isotope extraction either by leaching or by total fusion, which works because there is so much more meteoric  $^{10}\text{Be}$  than in situ  $^{10}\text{Be}$  in most samples. The resulting pure Be and Al are precipitated as hydroxide gels, heated to create oxides, and mixed with a metal powder (usually Nb) before measurement by accelerator mass spectrometry. All of this work is typically done in a clean room laboratory using fluorinated ethylene propylene labware to minimize contamination.

## Applications

Cosmogenic nuclides are used for dating landform exposure or deposition, estimating erosion rates, and tracing sediment sources. Each application relies on different assumptions, sampling strategies, and interpretation protocols.

### Erosion

The concentration of cosmogenic nuclides in bedrock outcrops, detrital river sediment, and soil reflects the long-term erosion rate of Earth's terrestrial surface. Accounting for the specific nuclide production rate at each sample site, higher concentrations of cosmogenic nuclides imply longer surface residence times for sample materials, and hence lower long-term erosion rates. Cosmogenic nuclides are effective erosion rate monitors because in situ cosmogenic nuclides are removed from outcrop surfaces by erosion, competing with the build-up of nuclides by cosmogenic production. In slowly eroding landscapes, rock remains in the nuclide production zone of Earth's surface for a longer period of time, and thus more nuclides accumulate; conversely, in rapidly eroding landscapes, there is only a short period of time for nuclides to accumulate before they are removed by erosion. This inverse relationship between near Earth-surface residence time and nuclide abundance drives geomorphologists' understanding of landscape dynamics through the measurement of cosmogenic nuclides.

How long term is a long-term erosion rate? That depends on the erosion rate. In the Himalayas, where erosion rates can be as high as 1 km/My, erosion is only integrated over a few millennia at most; in contrast, erosion rates in tectonically stable, arid regions such as much of central Australia may integrate erosion over millions of years. Measuring the concentration of cosmogenic nuclides in a bedrock outcrop quantifies the erosion rate of that outcrop's surface, whereas measuring cosmogenic nuclides in sediments quantifies the erosion rate of the drainage basin as a whole.

### Outcrop Erosion Rates

Early applications of cosmogenic nuclides demonstrated that some bedrock exposures in the arid and semiarid southern hemisphere were among the most stable in the world. In southern and central Australia, inselbergs (German for *island mountain*) stand prominently above otherwise featureless plains (Fig. 5). They appear to be losing mass by granular disintegration as well as the peeling of sheets of rock, centimeters to meters thick. Cosmogenic nuclide analysis of surface samples showed that many of these landforms were eroding at rates so slow (<0.5 m/My) that they had changed little since the Miocene time, some 20 Ma. Erosion rates this low have only been found in extremely water-deficient places such as the Dry Valleys of Antarctica and the Atacama Desert of northern Chile and southern Peru.



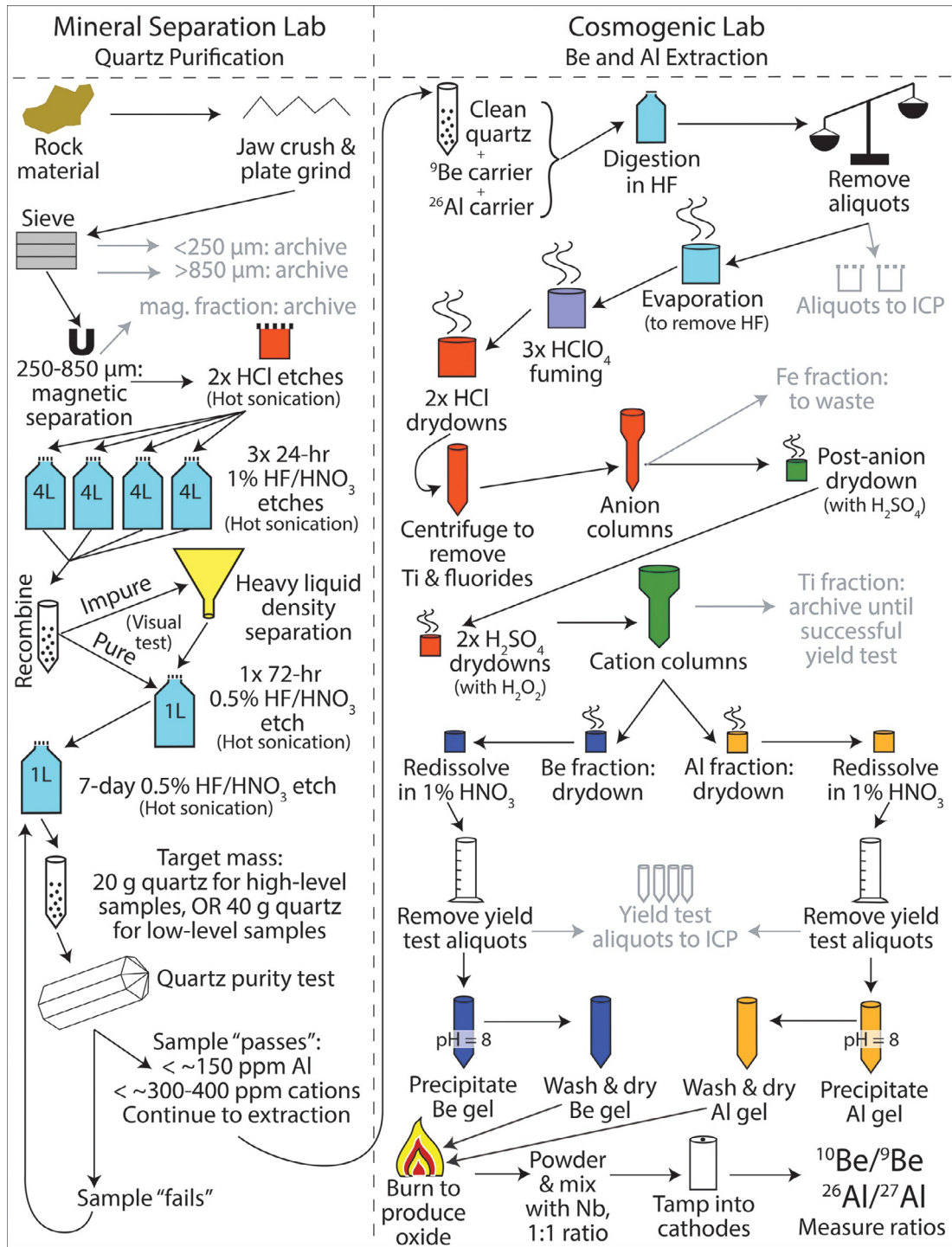


**Fig. 4** Flow chart of in situ  $^{10}\text{Be}/^{26}\text{Al}$  isotopic sample preparation methods. Arrows designate the direction of sample progression through the process, and gray font indicates sample fractions removed from the flow. Quartz preparation is described more fully in Kohl and Nishiizumi (1992). Modified from Corbett LB, Bierman, PR, and Rood DH (2016a) An approach for optimizing in situ cosmogenic  $^{10}\text{Be}$  sample preparation. *Quaternary Geochronology* 33: 24–34.

In less extreme environments at mid-latitudes, bedrock erosion occurs relatively more quickly at tens of meters per million years; at these rates, in situ  $^{10}\text{Be}$  integrates erosion over tens of thousands of years. Bedrock outcrops exist on the landscape because they erode more slowly than the hillslopes and river basins around them, and thus erosion rates derived from them should be considered minimum limits on the rate of landscape development through time. By contrast, in situ  $^{10}\text{Be}$  erosion rates derived from stream sediment samples are thought to reflect an average rate of landscape development. When paired together,  $^{10}\text{Be}$  erosion rates of bedrock outcrops and whole catchments for the same region can be compared, thus providing an estimate of relief generation



**Fig. 5** Weathering pit on the summit of Pildappa Rock, an inselberg on the Eyre Peninsula of South Australia. Erosion rates on the surface of this inselberg range between 40 and 50 cm/My likely the result of thin sheeting as shown at the bottom of the photo. The loss of large slabs as shown in the distance also removes mass from the surface of these landforms.

throughout the landscape. Such practices are often used as a means of assessing landscape stability and thus steady state erosion over millennial timescales.

Rates of bedrock erosion have been measured around the world although the data are spatially biased, particularly towards dry, arid environments because a minority of published bedrock erosion studies comprise a majority of the number of measured samples. Bedrock erosion in dry, arid environments (e.g., Namib Desert and southern Australia) are well represented in the literature; the temperate central Appalachian Mountains of the eastern United States are also well studied. Existing global bedrock  $^{10}\text{Be}$  erosion data suggest that sedimentary rocks erode faster than crystalline igneous or metamorphic rocks and that erosion rates are lowest in arid and polar environments. Whether these generalizations reflect true global drivers of outcrop erosion is uncertain owing to a clear spatial bias in the distribution of available data; only by acquiring new  $^{10}\text{Be}$  data in spatially under-sampled regions can such relationships be further understood.

### Basin-Averaged Erosion Rates

Measuring  $^{10}\text{Be}$  in bedrock outcrops estimates erosion at a single point on Earth's surface, but point-specific erosion rates are less useful for understanding landscape dynamics over large areas. To circumvent this limitation, geomorphologists measure the average concentration of  $^{10}\text{Be}$  extracted from a sample of river sand, typically in the 0.25–1 mm grain-size fraction. The average  $^{10}\text{Be}$  concentration of stream sand reflects nuclide production at all points upstream of the sample collection site. Thus, average measured nuclide concentrations yield an average erosion rate for the contributing drainage area. Catchment-averaged erosion rates interpreted from  $^{10}\text{Be}$  concentrations require several assumptions, the validity of which can be difficult to verify: (1) uniformity of quartz distribution and concentration in the watershed, (2) well-mixed river sediment, (3) rapid sediment transport time from

erosion to sample collection over geologically relevant timescales ( $10^2$ – $10^4$  year), and (5) sediment sourcing from gradual erosion of Earth's surface rather than pulsed denudation resulting from deep-seated landslides.

When these assumptions are reasonably met, basin-averaged erosion rates provide useful measurements of erosion over geologically recent timescales. In addition to measuring spatial and temporal patterns of erosion in landscapes globally, basin-averaged  $^{10}\text{Be}$  erosion rates have been used to locate seismic activity along faults, understand climatic and lithological controls on landscape development, assess landscape stability, determine sediment budgets, and provide context into the effects of human landscape practices on landscape development. However, this system is not useful for glacial landscapes, since glacial ice shields the sediments from nuclide production and also performs appreciable deep erosion.

Despite being applied to a larger geographical distribution, globally, relative to the distribution of bedrock erosion rates,  $^{10}\text{Be}$  has not been used as widely in tropical areas as in other parts of the world. Measuring in situ  $^{10}\text{Be}$  in quartz can be challenging in parts of the tropics that are formed by rocks with low quartz content, such as volcanic island arcs and carbonate marine platforms. In addition, abundant precipitation and warm temperatures lead to high rates of chemical denudation and aggressive chemical weathering. For example, in Cuba, measured concentrations of in situ  $^{10}\text{Be}$  in sediment are very high in some low-slope basins, reflecting long residence times near Earth's surface; however, chemical weathering rates exceed those inferred from  $^{10}\text{Be}$  and  $^{26}\text{Al}$  by an order of magnitude. This disagreement suggests that areas with deep weathering profiles, which are more likely in tectonically stable tropical locations, in situ  $^{10}\text{Be}$ -derived erosion rates may only represent minimum estimates of erosion unless chemical weathering is considered.

Global analyses of basin-averaged  $^{10}\text{Be}$  erosion rates suggest that mean basin hillslope angle and mean annual precipitation drive landscape evolution; which of these factors is the dominant factor seems to depend on whether the landscape is steep with high mean elevations (slope) or gentle topography with lower mean elevations (mean annual precipitation). As with bedrock erosion, basins underlain by sedimentary rock erode faster than those underlain by crystalline lithologies. Erosion rates are greatest in polar/alpine climates, likely owing to the presence of active glacial erosion and freeze-thaw fracturing; erosion rates are lowest in hyper-arid regions, such as the Atacama Desert. Overall, landscapes in tectonically active regions tend to erode more rapidly than those in tectonically quiescent regions, possibly driven by widespread occurrences of mass movements on oversteepened hillslopes, which deliver large volumes of sediment to rivers that come from depths greater than the cosmogenic nuclide production zone.

## Dating

Cosmogenic nuclides are used for determining the age of geologic events or landforms in two different ways: exposure age dating and burial dating. Simple exposure ages rely on the build-up of cosmogenic nuclides in samples at the Earth's surface at a known rate over time. In contrast, burial dating relies on burial and shielding from cosmic rays of the material being dated after initial surface exposure and the contrasting half-lives of at least two nuclides. Below, we focus on dating glacial events as an example; a similar approach can and has been used to date alluvial fan deposition, fault movements, and mass movements such as rockslides. Similar assumptions underlie any form of surface exposure dating: the sample of interest starts with a blank slate (no inherited nuclides), remains exposed, and has not been eroded since exposure. These assumptions are rarely 100% valid.

### Simple Glacial Dating

Cosmogenic nuclides have provided insight about glacial history and process since 1990. The most straightforward approach, simple exposure dating, involves using cosmogenic nuclide concentrations to quantify the amount of time that has elapsed since glaciers or ice sheets retreated and exposed the underlying landscape. Simple exposure dating relies on several assumptions: (1) This approach assumes a single, uninterrupted period of exposure, from which the nuclide concentrations can be interpreted as an exposure age following ice retreat or thinning. (2) Simple exposure dating assumes the surface has not been eroded or covered (e.g., by till or snow) during exposure, both of which would decrease nuclide production and thus concentrations and calculated exposure ages. (3) Simple exposure ages assume that the sampled surface does not contain any nuclides that accumulated during periods of prior exposure before the last deglaciation event.

Simple exposure dating has been used widely to constrain the timing and rates of glacial retreat across the world. In particular, exposure ages of boulders on a glacial moraine provide the age of the ice extent that deposited the boulders on the moraine.  $^{10}\text{Be}$  has been used to date boulders deposited by the Laurentide Ice Sheet, some of which form iconic New England landforms including Cape Cod and Martha's Vineyard. Dating moraines in sequence, such as up a glacial valley, can constrain retreat rate and history. However, moraines are actively eroding landforms, and thus interpretation of boulder ages may be complex. In addition to moraines, cosmogenic nuclides can be used to date the exposure of formerly glaciated bedrock or glacially deposited boulders to constrain the age and pace of ice retreat, even where moraines are absent. For example, exposure ages of bedrock and boulders now constrain the timing, pace, and pattern of ice retreat following the Last Glacial Maximum at several of Greenland's largest outlet glaciers.

Exposure ages of bedrock or glacially deposited boulders along an elevation transect on a formerly glaciated mountainside can quantify a vertical rate of ice thinning during deglaciation (Fig. 6). As an ice sheet thins and its surface lowers, higher elevations on mountains are exposed first while lower elevations are exposed later. Gradual changes in exposure age with elevation indicate slow ice thinning rates. Alternatively, similar exposure ages across horizontal and vertical distances often indicate very rapid ice loss that



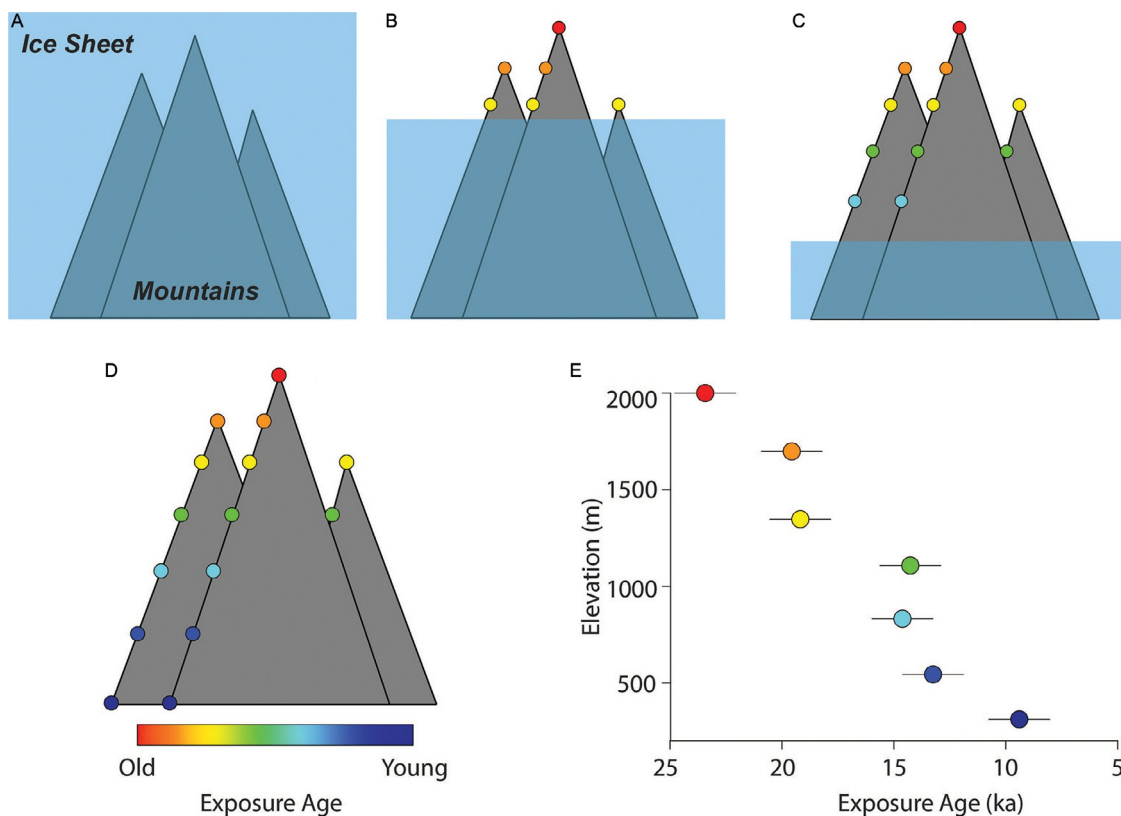


**Fig. 6** Schematic depiction of how in situ cosmogenic nuclides are used to constrain ice sheet thinning rates. In all panels, colored circles represent exposure ages of samples following the color scale in panel (D). Panels (A–C) show an ice sheet lowering around mountains, progressively exposing lower elevations over time as ice thins. Panel D shows the expected pattern of in situ cosmogenic nuclide exposure ages increasing with elevation on the deglaciated mountains. Panel E schematically shows the typical depiction of these data: a plot of  $^{10}\text{Be}$ -based exposure age and uncertainty on the  $x$ -axis and sample elevation on the  $y$ -axis. Regressions of these elevation-exposure age data reveal trends that represent rates of ice sheet thinning over time.

exposed the study area over a short period of time. This method has been used to constrain the thinning history of the Scandinavian, Antarctic, Greenland, and Laurentide Ice Sheets following the Last Glacial Maximum.

### Simple Burial Dating

The simplest burial dating involves measuring two cosmogenic nuclides in a single sample and calculating a burial age by comparing the measured nuclide ratio to the assumed ratio of the two nuclides at surface production which is thought, based on limited data, to be around 7.0. Such simple burial ages have been used to date old river gravels, offshore sediments, and cave deposits including those associated with the remains of early humans. Simple burial ages are beholden to a variety of assumptions, which can make them appear too old or too young. For example, muon production will create nuclides after burial making burial ages appear too young. If the sediment was deposited with a  $^{26}\text{Al}/^{10}\text{Be}$  ratio below the production ratio of 7, then the calculated age would be too old because some of the decay to lower the ratio would have occurred before deposition rather than after. For example, sediments from beneath the Greenland Ice Sheet have already experienced burial beneath ice, hence their  $^{26}\text{Al}/^{10}\text{Be}$  ratio is below 7; if the sediments are then buried in a terrace, the  $^{26}\text{Al}/^{10}\text{Be}$  ratio will continue to decrease, but the age of burial will appear old due to the prior burial beneath ice.

### Isochron Burial Dating

Cosmogenic isochron burial dating uses the post-burial decay of  $^{26}\text{Al}$  and  $^{10}\text{Be}$  to ascertain the timing of sediment deposition over an effective age range of 0.2 to 5 My. In the field, the isochron technique requires obtaining four or more quartz-bearing sediment samples (e.g., cobbles or different grain-size fractions) from a single stratigraphic horizon (indicative of common burial history). The sample horizon must be buried by several meters of sediment to shield sample material from most cosmic radiation and thus minimize post-burial nuclide production. The method assumes rapid and simultaneous burial of sample material. Careful fieldwork and stratigraphic interpretation are therefore mandatory, and several meters of massive sediment overlying the target

horizon is ideal. In the laboratory,  $^{26}\text{Al}$  and  $^{10}\text{Be}$  are determined separately in each subsample, making this a time-consuming and costly approach.

Computing an isochron burial age involves fitting a linear regression to measured isotope concentrations and uncertainties, with  $^{10}\text{Be}$  and  $^{26}\text{Al}$  on the x- and y-axes, respectively (Fig. 7). The slope of the regression (which decreases predictably over time) reflects the duration of post-burial decay from the surface  $^{26}\text{Al}/^{10}\text{Be}$  production ratio, and thus can be used to calculate the duration of burial. Unlike simple burial dating, where nuclide production by deeply penetrating muons can result in age underestimates, the isochron burial dating approach uses multiple samples with the same post-burial history. Thus, isochron burial dating minimizes sensitivity of the resulting age on post-burial production. This method requires no information about pre-burial sample history, identifies outlier samples that do not statistically overlap the linear fit to measured nuclide concentrations, and quantifies post-burial nuclide production as the y-intercept of the regression.

The isochron burial method can be used in many stratigraphic settings. For example, it has been used to constrain the age of hominid fossils buried in caves and to determine the rate of river downcutting from cave sediments isolated along gorge walls. Isochron dating is now commonly used to constrain the timing of river gravel deposition and terrace incision. This approach has recently been used to infer rates of river terrace uplift driven by tectonics in central Washington, and the rapid timing of tributary response at  $\sim 2.4$  Ma to the massive Yukon River capture event at the Pliocene–Pleistocene transition. Unique stratigraphy in China enabled a recent test of this method against traditional Ar dating of volcanic units above and below an isochron-dated gravel; stratigraphically consistent and statistically overlapping ages indicate the technique's robustness.

### Importance of Nuclide Inheritance for Dating

Nuclides inherited from prior episodes of near-surface exposure can complicate the interpretation of exposure ages (Fig. 8). In theory, surface exposure ages record the time following emplacement of a moraine, alluvial fan, or rock fall deposit, allowing for calculation of the timing of geologic or climatic events. In practice, many ages often vary widely across a single landform or exceed the expected or true depositional age. This scatter is likely due to inherited nuclides that accumulated during periods of prior exposure. These nuclides were not removed by erosion during transport or burial (e.g., by glacial ice). Issues of inheritance are particularly significant in areas where cold-based glaciers fail to achieve the ice thickness and basal ice temperatures required to produce meltwater and basal sliding, both of which allow for subglacial erosion, and therefore the removal of inherited nuclides in formerly exposed surfaces.

Antarctica is a perfect place to explore the impact of inherited nuclides on glacial exposure age chronologies. Stable, hyper-arid polar climate conditions along with relatively little tectonic activity, and subsequently low sub-aerial erosion rates ( $\sim 1$  m/My), have led to long-lived exposure of near-surface material. These surface materials are later covered and/or entrained by cold-based glacier ice that fails to erode and remove inherited nuclides. Subsequent ice advances may reincorporate these materials, perpetuating

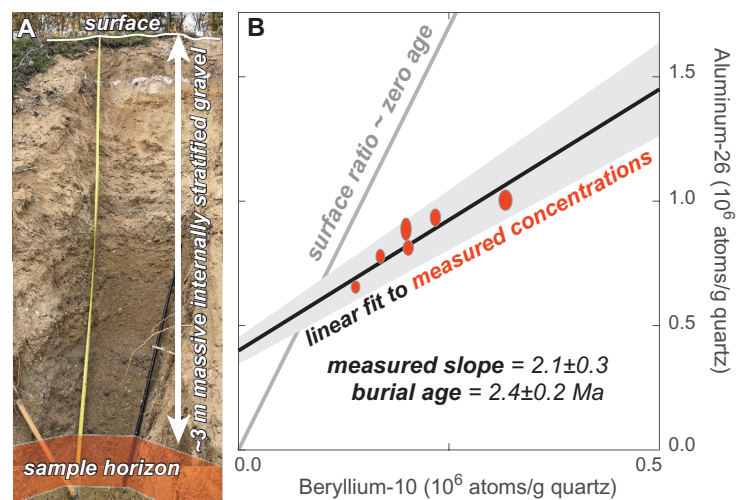
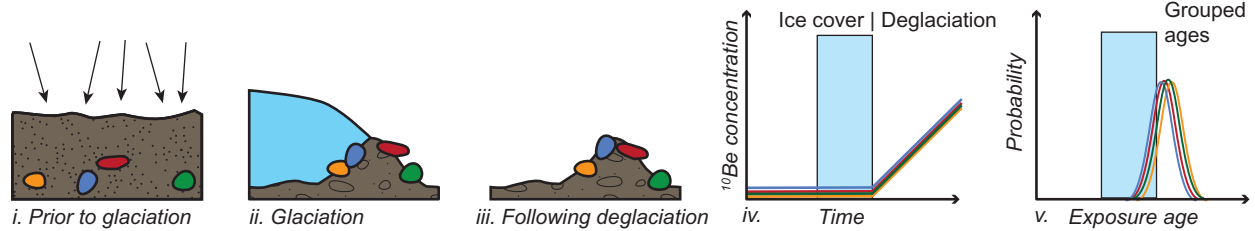


**Fig. 7** Isochron burial dating. (A) Isochron sample site in a Yukon River basin terrace gravel; the sample horizon is well-shielded from most cosmogenic radiation by several meters of overlying gravel. The massive gravel lacks stratigraphic unconformities that might indicate intervals of lesser shielding following the deposition of the sample horizon. (B) Isochron plot of aluminum-26 and beryllium-10 concentrations (red ellipses) from cobble, sand, and pebble samples obtained in the sample horizon depicted in (A) after Bender et al. (2018). The slope of the line fit to the measured concentrations is less than the slope of the surface production ratio and indicates post-burial nuclide decay equivalent to a burial age of  $\sim 2.4$  Ma. The elevated y-intercept reflects post-burial production equivalent to  $\sim 4 \times 10^5$  aluminum-26 atoms.

### A. Ideal scenario



### B. Prior exposure scenario

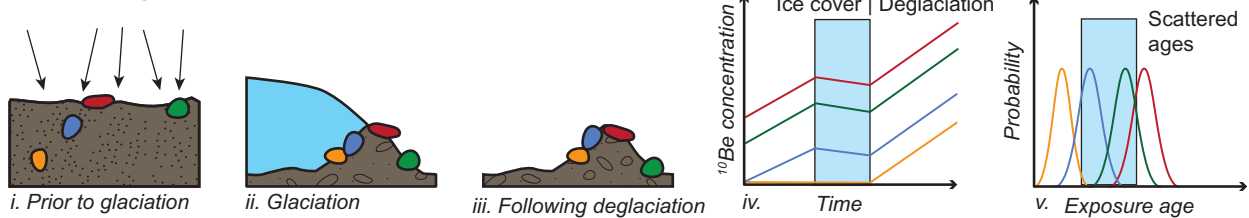


**Fig. 8** Effect of prior exposure upon exposure ages of boulder on glacial moraines adapted from Heyman et al. (2011). (A) In an ideal scenario, (i) boulders with no prior exposure are (ii) glacially transported and emplaced in a glacial moraine. Following deglaciation (iii) when boulders are exposed, (iv) the same inventory of  $^{10}\text{Be}$  atoms accumulates in each sample and (v) produces similar, grouped exposure ages that reliably record the timing of deglaciation. (B) If boulders are exposed on or just below the surface,  $^{10}\text{Be}$  is produced in surface boulders, but not deeper ones (i). The mixture of pre-exposed and non-exposed boulders are glacially transported and (ii) emplaced in a moraine and  $^{10}\text{Be}$  will decay when ice covered. Following deglaciation (iii)  $^{10}\text{Be}$  will accumulate in all boulders; however, some boulders will contain higher concentrations of  $^{10}\text{Be}$  inherited from prior exposure (iv). This results in (v) scattered exposure ages that do not constrain the timing of deglaciation.

nuclide inheritance through time. When the ice recedes and these rocks are deposited, the resulting exposure dataset is highly scattered with many ages that are ‘too old,’ sometimes on the order of hundreds of thousands of years. Accordingly,  $^{26}\text{Al}/^{10}\text{Be}$  ratios of such samples often indicate complex histories of repeated exposure and burial, although even using multiple nuclides in tandem does not provide a unique solution for the sample’s history. More recently, paired in situ  $^{14}\text{C}$  and  $^{10}\text{Be}$  exposure dating of glacial boulders has been used to date the age of deglaciation following the Last Glacial Maximum, as well as constrain the magnitude of prior exposure. This pairing can help detect inheritance in the longer-lived nuclide.

### Complex Exposure Histories

Complex exposure histories are prevalent in glaciated terrains and in some places make simple exposure dating unreliable. Several diagnostics are indicative of surfaces with inherited nuclides. In areas of cold-based ice, bedrock surfaces often have greater simple exposure ages than boulder surfaces because boulders can be plucked from areas of warm-based ice, transported glacially, and deposited in areas of cold-based ice. Low-elevation valley bottoms tend to be more eroded than high-elevation surfaces because thick ice and focused ice flow lead to effective erosion. Additionally, cold-based glacial ice can assemble boulders that may have experienced surface exposure during varying numbers of interglacial periods. As a result, boulder ages often form multimodal age distributions (Fig. 9). Finally, different cosmogenic nuclides have different half-lives; hence, for surfaces that have been subjected to burial, the shorter-lived nuclide (i.e.,  $^{26}\text{Al}$ ) decays more rapidly than the longer-lived nuclide (i.e.,  $^{10}\text{Be}$ ), causing a disagreement in simple exposure ages from different nuclides.

Measuring multiple nuclides in tandem can constrain the relative proportions of exposure and burial durations in a surface covered by non-erosive ice (Fig. 10). When exposure begins on a fresh surface, the  $^{26}\text{Al}/^{10}\text{Be}$  ratio matches the production ratio of the two nuclides. If a previously exposed surface is buried and shielded from further nuclide production, the  $^{26}\text{Al}/^{10}\text{Be}$  ratio drops because the half-life of  $^{26}\text{Al}$  is less than the half-life of  $^{10}\text{Be}$ . If a sample is exposed again following burial, production resumes and the  $^{26}\text{Al}/^{10}\text{Be}$  ratio increases because the production rate of  $^{26}\text{Al}$  is greater than that of  $^{10}\text{Be}$ . Using data from paired cosmogenic isotopes, a minimum-limiting history can be calculated for the simplest possible scenario: one period of exposure followed by one period of burial. However, minimum-limiting exposure/burial durations calculated with paired isotopes can significantly underestimate the sample’s true history, especially if the sample has experienced numerous exposure/burial cycles.

Any inferences stemming from  $^{26}\text{Al}/^{10}\text{Be}$  ratios depend in part upon the assumed  $^{26}\text{Al}/^{10}\text{Be}$  production ratio, which is a direct function of the production rates of the two nuclides. Until recently, the  $^{26}\text{Al}$  and  $^{10}\text{Be}$  production ratio was assumed to be 6.75 globally. However, recent work suggests that the production ratio is itself dependent on latitude and elevation because each isotope’s production rate scales differently. Some studies present data suggesting that the production ratio can be greater than 6.75, with values ranging as high as  $\sim 7.3$ . High-latitude regions appear most likely to have higher production ratios.

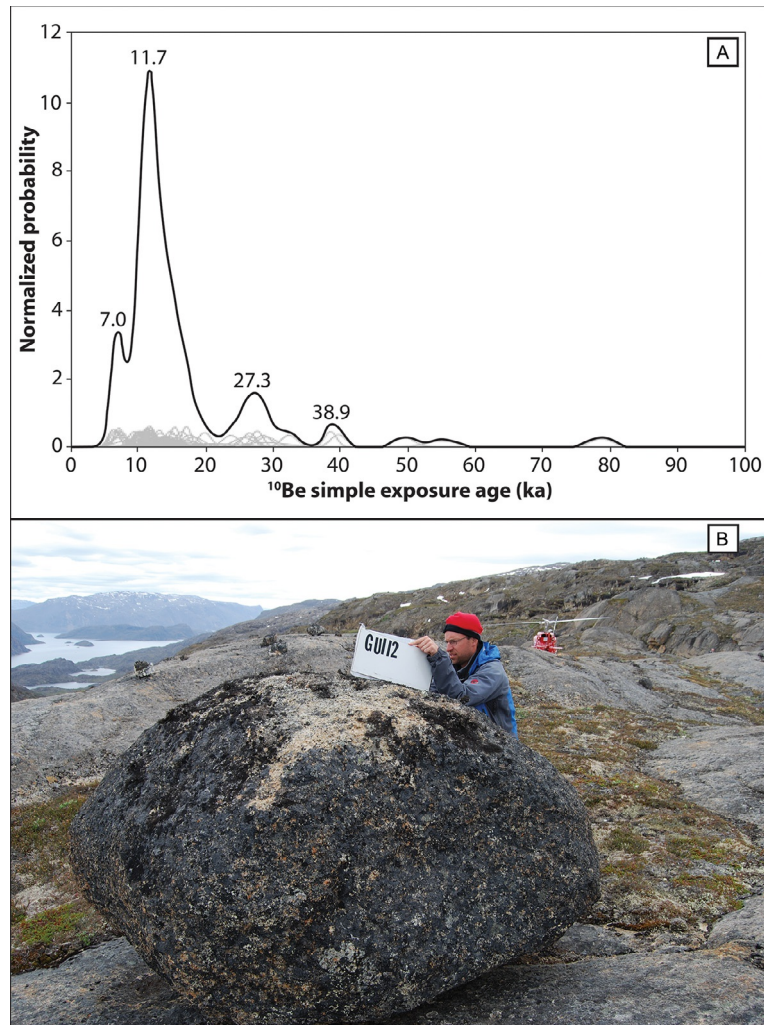


**Fig. 9** Complexities of cosmogenic dating in a landscape dominated by cold-based ice. (A) Example probability density function of boulder  $^{10}\text{Be}$  ages from a cold based ice landscape. These data are from southern Baffin Island (Corbett et al., 2016b) and include 82 ages. Thin gray lines represent the measured isotopic concentrations and internal uncertainties for each sample; the thick black line represents the summed probability. Prominent peaks are labeled by age (in thousands of years ago, ka), with the young peak ( $\sim 11$  ka) corresponding to the deglaciation age of the landscape. (B) Photograph of a heavily weathered boulder from Upernavik, northwestern Greenland. This boulder has a  $^{10}\text{Be}$  exposure age of  $\sim 20$  ka (Corbett et al., 2013) due to the presence of inherited  $^{10}\text{Be}$ , even though the landscape was likely deglaciated  $\sim 11$  ka based on other data.

### Sediment Sourcing and Tracing

Although cosmogenic nuclides are commonly thought of as tools for dating and deciphering long-term rates of erosion, they are also powerful means for inferring the distribution and speed of surface processes. In this context, isotopes are used as tracers to determine sediment sources and the rate at which sediment moves across the landscape.

For example, the Waipaoa Basin on the North Island of New Zealand is rapidly eroding. Massive landslides tear into the poorly consolidated sandstone and mudstone hillslopes filling the channel with sediment. There are significant management questions about how to handle sediment loads so extreme that channels aggrade, burying bridges. With so little quartz-bearing sand and such high erosion rates, measuring in situ  $^{10}\text{Be}$  is challenging but meteoric  $^{10}\text{Be}$  is easily detected. With such measurements and a stream network analysis using many samples of river sediment, it becomes clear that one very large landslide, which contributed deeply excavated sediment containing very low concentrations of meteoric  $^{10}\text{Be}$ , dominates the sediment flux into and out of the basin. Such sediment tracing requires end-member sediment sources with different characteristic  $^{10}\text{Be}$  concentrations and a network analysis to determine how  $^{10}\text{Be}$  changes downstream. Such work is by no means limited to humid regions dominated by landslides; it has also been used to trace the source of sediment in ephemeral dry land streams in North America and the Middle East and to trace the effects of European colonization on topsoil erosion in North America and Australia.

In a very different setting, arid Mojave Desert of southwestern North America, in situ  $^{10}\text{Be}$  was used to trace sediment as it moves out of steep drainage basins and down low-gradient desert piedmonts. By sampling ephemeral stream sediment as it left the basins



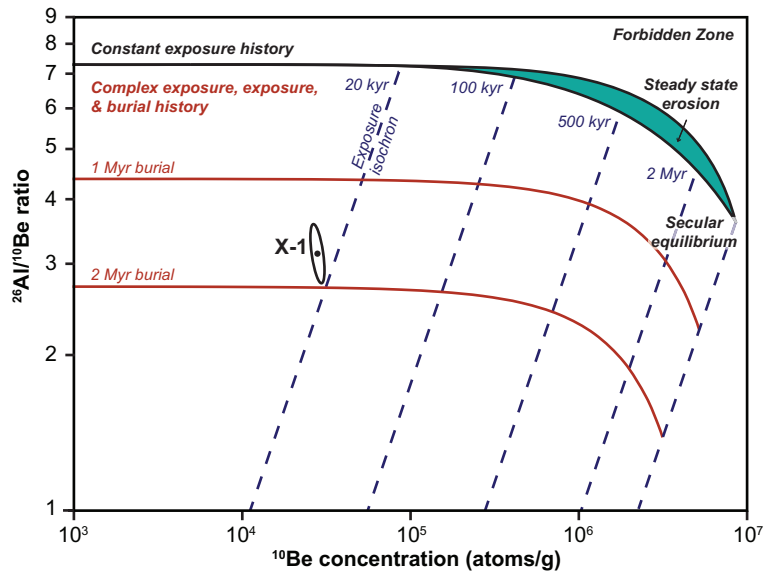


**Fig. 10**  $^{26}\text{Al}$  and  $^{10}\text{Be}$  two isotope diagram. Material with a constant exposure history will plot along the upper black line until  $^{10}\text{Be}$  and  $^{26}\text{Al}$  concentrations reach secular equilibrium where the production rate is offset by radioactive decay. Material undergoing steady state erosion, where the removal of nuclides is balanced by production, will plot in the island of steady state erosion (green area). If material is exposed and then eroded or buried, it will yield a complex exposure history that plots anywhere below the black lines of constant exposure or island of steady state erosion. Lower  $^{26}\text{Al}/^{10}\text{Be}$  ratios indicate longer duration of burial. For example, theoretical sample X-1 (ellipse shows  $^{26}\text{Al}$  and  $^{10}\text{Be}$  measurement uncertainties) was exposed for  $\sim 20$  ky and buried for at least 1.8 My.

and then using amalgamated samples collected along slope-parallel transects at increasing distances from the range front, it is possible to map an increase in in situ  $^{10}\text{Be}$  concentration downslope. Combining isotopic measurements with field observations of a mixed, active layer about 50 cm deep, a simple mathematical model calculates the average sediment speeds down the piedmont of centimeters to decimeters per year. Long-term rates of sediment movement matched well with short-term rates determined using pebble tracking over just a few years.

### Storms, Wet Seasons, and Reproducibility Over Time

Although erosion rate measurements are based upon the assumption that the concentration of cosmogenic nuclides in river sediment are steady over time (so it does not matter when samples are collected), there is evidence that sediment comes from different parts of the landscape during big storms or seasonally, such as the wet and dry season in regions with extreme seasonal variability in rainfall. Replicate measurements (samples taken at the same place at different times) of in situ and meteoric  $^{10}\text{Be}$  demonstrate that although samples taken at two times at the same site have similar median values, individual samples replicate poorly, especially in places with erosion characterized by landslides, steep topography, concentrated farming, or intense rainfall (Fig. 11).

Large events like hurricanes can change apparent erosion rates determined from sediment collected before and after a storm, in single basins. For example, on the small Caribbean island of Dominica, a comparison of samples collected before and after the Category 5 Hurricane Maria in 2017 demonstrated that although individual sample pairs from the same basin replicated poorly, the dataset replicated well. In this case, no strong trends in what types of areas replicated better were observed, except that areas with extensive farming and landsliding seemed to replicate less well. In addition, the correlation between erosion rates and landscape parameters (such as steepness) are different before and after the storm.

In a time-series analysis of sample replicability in two small watersheds ( $<4$  km<sup>2</sup>) in Puerto Rico following Hurricane Maria, the watershed with a major landslide upstream had isotope concentrations that were initially low and increased linearly over approximately 18 months compared to concentrations in sediment from the other, unaffected watershed. Together, these data suggest that in areas with deep weathering and large storms, such as hurricanes, erosion rates taken from a single sample could be biased by sampling soon after a storm. This bias is the result of sediment sourced from deep below the surface by landslides. Some data reproduce well before and after large storms, such as the comparable  $^{10}\text{Be}$  concentrations measured along the trunk and tributaries of the much larger Boulder Canyon (Colorado, USA) following severe flooding in 2013. Here,  $^{10}\text{Be}$  concentrations were comparable to those measured before the flood despite significant wildfires in one of the tributaries.

Another fundamental assumption underlying erosion rate measurement from  $^{10}\text{Be}$  is that sediment from the upstream watershed is well mixed; some environments have sediment that is poorly mixed and violates this assumption. Samples are poorly mixed when sediment is taken too close to the junction with a tributary, when one basin has experienced a major erosion event (such as a landslide), or when basins are very small. When basins are larger and erosion rates are faster (thus contributing more

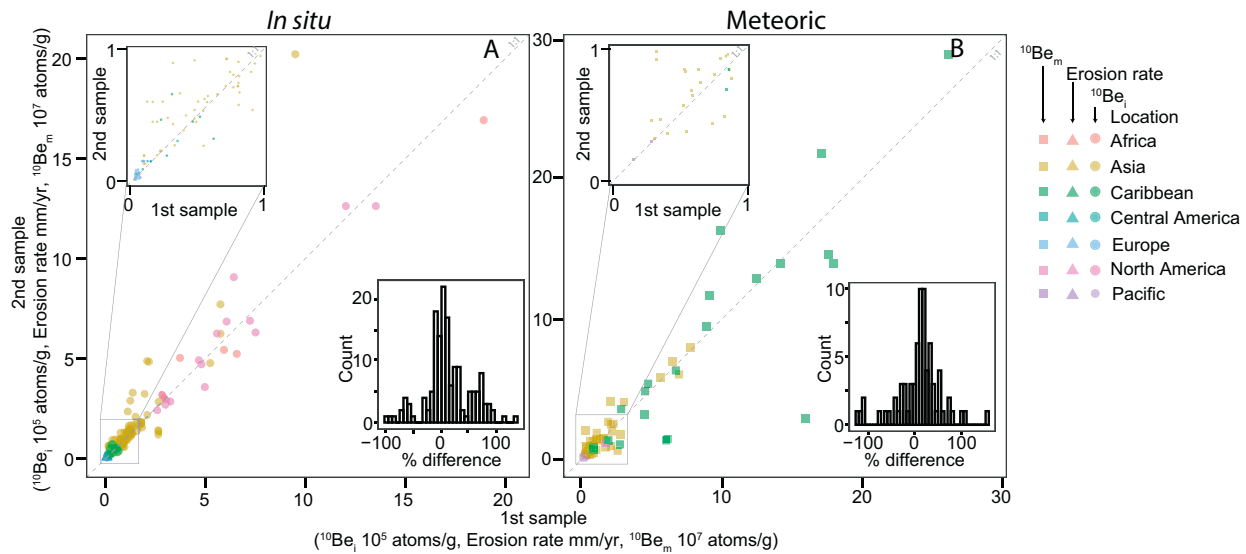


**Fig. 11** Global compilation of samples taken at the same place at two different times and analyzed for in situ (A) and/or meteoric (B)  $^{10}\text{Be}$ . Inset on upper left enlarges the area from 0 to 1, on lower right inset shows distribution of the percent change between samples taken at two different time periods. Colors indicate sample location while shape indicates parameter plotted. Triangles showing erosion rate measurements are clustered in the lower left corner of the in situ plots in (A). This is because the erosion rates were all measured in a relatively slowly eroding part of Europe and are  $<0.1$  mm/year. These sites have erosion rates shown rather than in situ concentration because replicate pairs are not located at exactly the same place. Figure after Sosa Gonzalez V, Schmidt AH, Bierman PR, and Rood DH (2017). Spatial and temporal replicability of meteoric and in situ  $^{10}\text{Be}$  concentrations in fluvial sediment. *Earth Surface Processes and Landforms* 42: 2570–2584.

sediment), samples are typically better mixed. If basins become too large and contain deep and wide floodplains where sediment storage is long, such as the Amazon River basin,  $^{10}\text{Be}$  concentrations in sediment at the mouth of a large river may better reflect  $^{10}\text{Be}$  concentrations of steep, mountainous headwater catchments than erosion across the entirety of the floodplain.

### Analysis of Deep-Sea Sediment

Deep sea sediments provide a way of looking back in time. Marine archives have been cored repeatedly by series of international ocean drilling collaborations. Although sample volumes are constrained by the diameter of the core and temporal resolution is limited by low sedimentation rates typical of many marine settings, marine cores are usually independently dated allowing measured  $^{10}\text{Be}$  concentrations to be decay corrected to the time of deposition.

Cosmogenic nuclide analysis of marine sediment has determined the prior exposure and erosion history of Greenland and Antarctica. Extremely low measured concentrations of  $^{10}\text{Be}$  and  $^{26}\text{Al}$  suggested that much of Antarctica had not been exposed (and thus deglaciated) for many millions of years. In contrast, data from ocean bottom sediment around Greenland, which had  $^{10}\text{Be}$  and  $^{26}\text{Al}$  concentrations higher than that from near Antarctica, tell a different story of spatially variable erosion and occasional deglaciation of the island during Pliocene and Pleistocene time.

Comparing  $^{10}\text{Be}$  and  $^{26}\text{Al}$  from deep sea sediment with more proximal cosmogenic records of glacial erosion and surface exposure helps better constrain the history of continental ice sheets. In central Greenland,  $^{10}\text{Be}$  and  $^{26}\text{Al}$  concentrations measured in bedrock at the bottom of the Greenland Ice Sheet Project 2 (GISP2) ice core site mandate deglaciation during the Pleistocene, which suggests the Greenland Ice Sheet formed, disappeared, and reformed in the recent geologic past—the last million years. This is important because the Greenland Ice Sheet must have melted when the concentration of carbon dioxide in the atmosphere was no more than 300 ppm. In 2020, atmospheric carbon dioxide levels are almost 420 ppm.

### What Will the Future Bring?

Cosmogenic nuclides have allowed geoscientists to understand the rates of surface processes and the dates of some landforms in a way only dreamed of several decades ago. As a community, we can now better constrain the timing of climatic and tectonic landscape changes, the rate at which sediment is generated and landscapes erode, and the source of material moving down rivers. Measuring basin-scale rates of erosion and dating moraines has become commonplace. The challenge now is to think differently and come up with new and innovative ways to apply these isotopes to better understand Earth as a dynamic system, especially as climate change and human activities increasingly change our planet's surface.

Advances in laboratory procedures and analytical instruments have increased the sensitivity of isotope analyses and thus the minimum exposure time needed before an age can be calculated. As we move forward, picking the right problem, in the right place, and applying the right sampling strategy will be key to getting new and interesting data about how Earth works from isotopes created by particles that have traveled from light years away.

## Further Reading

- Balco G (2011) Contributions and unrealized potential contributions of cosmogenic-nuclide exposure dating to glacier chronology, 1990–2010. *Quaternary Science Reviews* 30: 3–27.
- Balco G and Rovey CW (2008) An isochron method for cosmogenic-nuclide dating of buried soils and sediments. *American Journal of Science* 308: 1083–1114.
- Bender AM, Amos CB, Bierman P, Rood DH, Staisch L, Kelsey H, and Sherrod B (2016) Differential uplift and incision of the Yakima River terraces, central Washington State. *Journal of Geophysical Research, Solid Earth* 121: 365–384.
- Bender AM, Lease RO, Corbett LB, Bierman P, and Caffee MW (2018) Ongoing bedrock incision of the Fortymile River driven by Pliocene–Pleistocene Yukon River capture, eastern Alaska, USA, and Yukon, Canada. *Geology* 46: 635–638.
- Brown ET, Stallard RF, Larsen MC, Raisbeck GM, and Yiou F (1995) Denudation rates determined from the accumulation of in situ-produced  $^{10}\text{Be}$  in the Luquillo Experimental Forest, Puerto Rico. *Earth and Planetary Science Letters* 129: 193–202.
- von Blanckenburg F and Willenbring JK (2014) Cosmogenic nuclides: Dates and rates of Earth-surface change. *Elements* 10: 341–346.
- Corbett LB, Bierman PR, Graly JA, Neumann TA, and Rood DH (2013) Constraining landscape history and glacial erosivity using paired cosmogenic nuclides in Upernavik, northwest Greenland. *GSA Bulletin* 125: 1539–1553.
- Corbett LB, Bierman PR, and Rood DH (2016a) An approach for optimizing in situ cosmogenic  $^{10}\text{Be}$  sample preparation. *Quaternary Geochronology* 33: 24–34.
- Corbett LB, Bierman PR, and Davis PT (2016b) Glacial history and landscape evolution of southern Cumberland Peninsula, Baffin Island, Canada, constrained by cosmogenic  $^{10}\text{Be}$  and  $^{26}\text{Al}$ . *GSA Bulletin* 128: 1173–1192.
- Dickin AP (2018) *Radiogenic Isotope Geology*. Cambridge University Press.
- Dunai T (2010) *Cosmogenic Nuclides: Principles, Concepts and Applications in the Earth Surface Sciences*. Cambridge: Cambridge University Press.
- Faure G and Mensing TM (2005) *Isotopes: Principles and Applications*. John Wiley & Sons.
- Gosse JC and Phillips FM (2001) Terrestrial in situ cosmogenic nuclides: Theory and application. *Quaternary Science Reviews* 20: 1475–1560.
- Graly JA, Bierman PR, Reusser LJ, and Pavich MJ (2010) Meteoric  $^{10}\text{Be}$  in soil profiles—A global meta-analysis. *Geochimica et Cosmochimica Acta* 74: 6814–6829.
- Granger D (2006) A review of burial dating methods using  $^{26}\text{Al}$  and  $^{10}\text{Be}$ . *Geological Society of America Special Papers* 415: 1–16.
- Heyman J, Stroeven A, Harbor J, and Caffee M (2011) Too young or too old: Evaluating cosmogenic exposure dating based on an analysis of compiled boulder exposure ages. *Earth and Planetary Science Letters* 302: 71–80.
- Kohl CP and Nishizumi K (1992) Chemical isolation of quartz for measurement of in-situ-produced cosmogenic nuclides. *Geochimica et Cosmochimica Acta* 56: 3583–3587.
- Lal D (1991) Cosmic ray labeling of erosion surfaces: In situ nuclide production. *Earth and Planetary Science Letters* 104: 424–439.
- Portenga EW and Bierman P (2011) Understanding Earth's eroding surface with  $^{10}\text{Be}$ . *GSA Today* 21: 4–10.
- Sosa Gonzalez V, Schmidt AH, Bierman PR, and Rood DH (2017) Spatial and temporal replicability of meteoric and in situ  $^{10}\text{Be}$  concentrations in fluvial sediment. *Earth Surface Processes and Landforms* 42: 2570–2584.
- Zhao Z, Granger DE, Chen Y, Shu Q, Liu G, Zhang M, Hu X, Wu Q, Hu E, Li Y, and Yan Y (2017) Cosmogenic nuclide burial dating of an alluvial conglomerate sequence: An example from the Hexi Corridor, NE Tibetan Plateau. *Quaternary Geochronology* 39: 68–78.

## Relevant Websites

- <https://depts.washington.edu/cosmolab/>.
- [http://www.iceandclimate.nbi.ku.dk/research/past\\_atmos/cosmogenic\\_isotopes/](http://www.iceandclimate.nbi.ku.dk/research/past_atmos/cosmogenic_isotopes/).
- [https://www.physics.purdue.edu/primelab/introduction/cosmogenic\\_nuclides.html](https://www.physics.purdue.edu/primelab/introduction/cosmogenic_nuclides.html).
- <http://www.uvm.edu/cosmolab/>.